Title
Moving beyond Fine Particle Mass: High-Spatial Resolution Exposure to Source-Resolved Atmospheric Particle Number and Chemical Mixing State

Journal
Environmental Health Perspectives, 128(1)

ISSN
1542-4359

Authors
Ye, Qing
Li, Hugh Z
Gu, Peishi
et al.

Publication Date
2020

DOI
10.1289/ehp5311

Peer reviewed

A Section 508–conformant HTML version of this article is available at https://doi.org/10.1289/EHP5311.

Moving beyond Fine Particle Mass: High-Spatial Resolution Exposure to Source-Resolved Atmospheric Particle Number and Chemical Mixing State

Qing Ye,[1] Hugh Z. Li,[1,2*] Peishi Gu,[1,2] Ellis S. Robinson,[1,2] Joshua S. Apte,[3] Ryan C. Sullivan,[1,2] Allen L. Robinson,[1,2] Neil M. Donahue,[1] and Albert A. Presto[1,2]*

[1]Center for Atmospheric Particle Studies, Carnegie Mellon University, Pittsburgh, Pennsylvania, USA
[2]Department of Mechanical Engineering, Carnegie Mellon University, Pittsburgh, Pennsylvania, USA
[3]Department of Civil, Architectural, and Environmental Engineering, University of Texas at Austin, Austin, Texas, USA

Background: Most epidemiological studies address health effects of atmospheric particulate matter (PM) using mass-based measurements as exposure surrogates. However, this approach ignores many critical physiochemical properties of individual atmospheric particles. These properties control the deposition of particles in the human lung and likely their toxicity; in addition, they likely have larger spatial variability than PM mass.

Objectives: This study was designed to quantify the spatial variability in number, size, source, and chemical mixing state of individual particles in a populous urban area. We quantified the population exposure to these detailed particle properties and compared them to mass-based exposures.

Methods: We performed mobile sampling using an advanced single-particle mass spectrometer to measure the spatial variability of number concentration of source-resolved 50–1,000 nm particles and particle mixing state in Pittsburgh, Pennsylvania. We built land-use regression (LUR) models to estimate their spatial patterns and coupled them with demographic data to estimate population exposure.

Results: Particle number concentration had a much larger spatial variability than mass concentration within the city. Freshly emitted particles from traffic and cooking drive the variability in particle number, but mass concentrations are dominated by aged background particles composed of secondary materials. In addition, people exposed to elevated number concentrations of atmospheric particles are also exposed to more externally mixed particles.

Conclusions: Our advanced measurement technique provides a new exposure picture that resolves the large intra-city spatial heterogeneity in traffic and cooking particle number concentrations in the populous urban area. Our results provide a complementary and more detailed perspective compared with bulk measurements of composition. In addition, given the influence of particle mixing state on properties such as particle deposition in the lung, the large spatial gradients of chemical mixing state may significantly influence the health effects of fine PM. https://doi.org/10.1289/EHP5311

Introduction

Exposure to atmospheric particles, or particulate matter (PM), is associated with chronic and acute health effects such as premature death, cardiorespiratory morbidity, and increased daily hospital admissions (e.g., Hamra et al. 2014; Pope and Dockery 2006; Samet et al. 2000). Atmospheric particles have diverse physiochemical properties that determine their environmental fate and their interaction with human bodies. Therefore, a detailed and thorough characterization of individual atmospheric particles is essential to understand proper dose metrics for associated health effects (Cassee et al. 2013).

Conventional PM exposure studies rely on bulk measurement techniques such as collecting particles onto substrates (filters) to determine total mass concentration (e.g., Eeftens et al. 2012; Hamra et al. 2014; Samet et al. 2000). These types of mass measurements are easy to conduct and can provide trace elemental composition using techniques such as X-ray fluorescence (Herner et al. 2006; Landis et al. 2001). However, they only provide bulk data on the entire particle population. In the atmosphere, a particle population comprises hundreds to tens of thousands of individual particles per cubic centimeter. It is difficult to disaggregate bulk mass data into atmospherically relevant groups that differ in physiochemical characteristics of individual particles. This is an issue because particles emitted from different sources have different properties (Li et al. 2018; Miguel et al. 1998; Shields et al. 2007). Measuring the physiochemical differences is critical in order to identify the sources responsible for elevated exposure levels and health effects because emissions in populous urban areas are highly inhomogeneous and dynamic (Fuzzi et al. 2015; Mohr et al. 2011).

Figure 1 presents a conceptual illustration of what filter data (or other types of mass-based bulk measurements) miss for estimating intra-city exposure contrasts. In the atmosphere, different particles carry different chemical fingerprints and different sizes depending on their sources. In high source–impact locations such as urban centers, freshly emitted particles directly emitted by sources are more numerous than background particles, which mainly comprise secondary species formed from atmospheric chemistry. In downwind suburban areas with low emissions, the number concentration of freshly emitted particles greatly decreases. Freshly emitted particles are often smaller than background particles that have undergone substantial atmospheric processing, a process which grows particles via coagulation and condensation of secondary materials (Seinfeld and Pandis 2016). Therefore, freshly emitted particles are generally minor contributors to PM mass but may be major contributors to particle number, depending on the location. Mass-based measurements only provide total PM mass and chemically resolved mass from further analysis, with no information on individual particle characteristics such as size, number concentration, and composition. Individual particles are what deposit in the lung, not the bulk particle mass collected on a filter. The properties of these individual particles control their deposition characteristics and likely their toxicity. Therefore, improved knowledge of individual particle properties is likely important for developing a mechanistic understanding of the causes of health effects associated with PM. In addition, relying solely on mass

*These authors contributed equally to this manuscript.
Address correspondence to Albert A. Presto, Doherty Hall 2115, 5000 Forbes Ave., Pittsburgh, PA 15213 USA. Telephone: (412) 721-5203. Email: apresto@andrew.cmu.edu, or Neil M. Donahue, Doherty Hall 2116, 5000 Forbes Ave., Pittsburgh, PA 15213 USA. Telephone: (412) 268-4415. Email: nmd@andrew.cmu.edu

Supplemental Material is available online (https://doi.org/10.1289/EHP5311).
The authors declare they have no actual or potential competing financial interests.
Received 14 March 2019; Revised 22 October 2019; Accepted 6 December 2019; Published 14 January 2020.

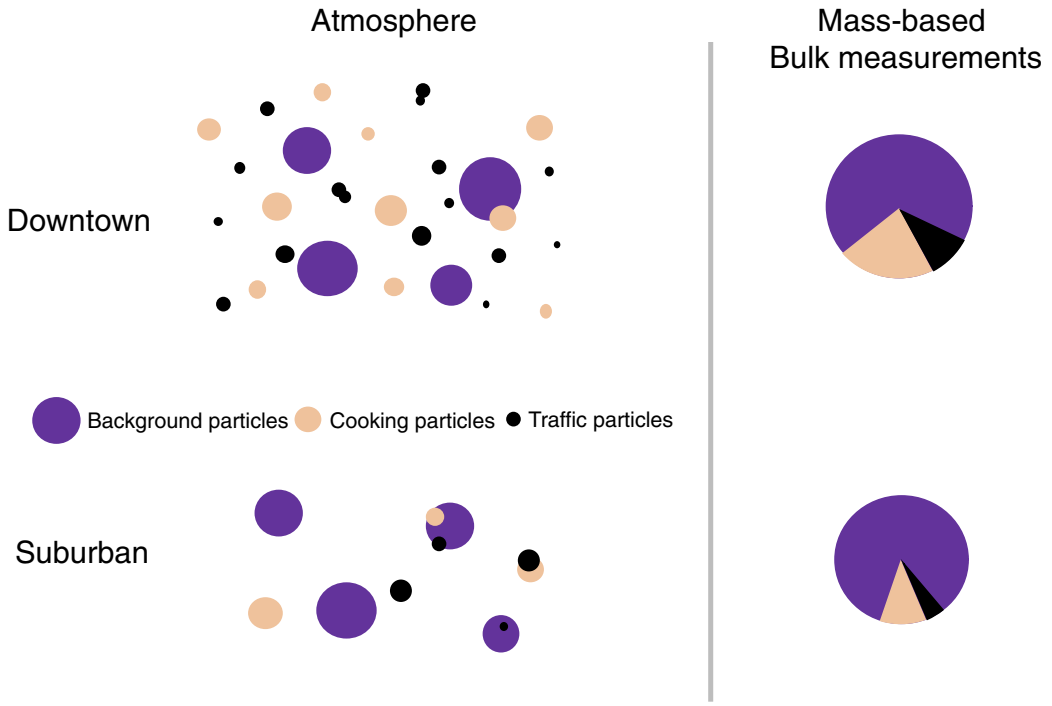

Figure 1. A conceptual illustration of PM in the atmosphere versus traditional mass-based bulk measurements of fine particle pollution. Different colors represent particles from different sources with different chemical composition. Conventional bulk measurements provide only total mass information. Some may provide mass-based contribution from different chemical constituents after further analysis. Such measurements are blind to particle physiochemical properties such as number concentration, size, and chemical mixing state. Although the total mass loadings may be similar, these properties differ greatly between highly source-active areas such as downtown and suburban areas low in emission sources in which particles have experienced greater extents of atmospheric processing. These properties potentially have important health implications, but it is difficult to use bulk measurements to capture the associated exposure variability.

concentration for human exposure estimates conceals the intra-city spatial heterogeneity of particle populations because most of the mass is dominated by background particles whose pollution patterns are regional (Robinson et al. 2007).

Growing evidence suggests that number concentrations of ultrafine or submicrometer particles are an important indicator for adverse health effects (Baldauf et al. 2016; Downward et al. 2018; Ostro et al. 2015; Penttinen et al. 2001; Wittmaack 2007) due to their large surface-to-volume ratio and their high efficiency to deposit into the deeper respiratory system. Particle number measurements typically use optical particle counters, which do not resolve composition (and therefore sources). As a result, spatial models [e.g., land-use regressions (LURs)] have major challenges in accurately predicting particle number concentration (Kerckhoffs et al. 2016; Patton et al. 2015; Saraswat et al. 2013) given that the sources of the particles are largely undetermined. Some studies have used methods such as positive matrix factorization to reveal important sources for particle number concentration (Kim et al. 2004; Sowlat et al. 2016; Squizzato et al. 2019), but these studies often rely on a limited number of stationary sites and therefore may not capture the intra-city spatial patterns of population exposure.

The mixing state is a micro-scale chemical property commonly used to describe the heterogeneity in chemical composition of individual particles across a particle population. Bulk measurements cannot resolve the chemical mixing state of atmospheric particles. In an externally mixed population, individual particles have different chemical compositions. This usually indicates that particles are emitted by different sources, similar to the downtown atmosphere depicted in Figure 1, where particle number concentrations are dominated by freshly emitted particles from various sources. In contrast, in downwind areas or background regions, each particle has more similar chemical composition (internally mixed) due to atmospheric processing that homogenizes chemical composition (Moffet et al. 2008; Robinson et al. 2016).

The mixing state may affect particle-health associations because it changes particle properties such as water solubility and deposition efficiency in the respiratory tract (Ching and Kajino 2018). In addition, different chemical species in individual particles may interact synergistically after being inhaled (Freedman et al. 2019; Highwood and Kinnersley 2006; Wilson et al. 2002). Therefore, it is likely that some of the reported inter-city heterogeneity in PM health effects (Franklin et al. 2007) is due to differences in mixing state. Particle mixing state changes greatly in areas with different emission activities (Ye et al. 2018). However, previous studies have not characterized the variability of exposure to particle mixing state, so it is difficult to assess its association with PM health effects.

Advanced single-particle mass spectrometers, which measure real-time size and chemical composition of individual particles with high sensitivity and time resolution, have been widely used to understand atmospheric chemical processes (Cross et al. 2007; Sullivan and Prather 2005; Ye et al. 2018; Zelenyuk and Imre 2005). Because particle physiochemical properties are measured on the single-particle basis, one can disaggregate the entire population into subgroups of particles from different sources. In addition, the chemical mixing state can also be readily computed by quantifying the varieties of species constituting individual particles and in the entire population.

In this study, we first present state-of-the-art single-particle measurements to characterize and quantify intra-city spatial variabilities of source-resolved particle number and chemical mixing state in various locations in a metropolitan area. We then build LUR models (Hoek et al. 2008) to predict their spatial patterns. We combine the predicted concentrations with

U.S. Census (https://www.census.gov/geographies/reference-maps/2010/geo/2010-census-tract-maps.html) block group data to investigate fine spatial scale population exposure to source-resolved particles with the integration of chemical mixing state. We finally compare source-resolved particle number and mass concentrations, suggesting the need to incorporate more physiochemical details of PM in future health studies.

Methods

Study Area and Mobile Sampling

We conducted *in situ* atmospheric measurements in Pittsburgh, Pennsylvania, and its surrounding suburban areas in Allegheny County from August 2016 to February 2017. Pittsburgh is located at the confluence of three rivers—the Allegheny, Ohio, and Monongahela—with a complex topography with rivers, hills, and valleys. The region has longstanding air pollution problems that are caused by complex sources from local industrial activities, vehicular emissions, commercial activities, transported power-plant emissions, and other regional emissions (Wittig et al. 2004). Recent air-quality measurements in Pittsburgh have showed that the dominant anthropogenic sources of urban PM are emissions from traffic and restaurant cooking (Gu et al. 2018; Robinson et al. 2018).

We performed highly spatially resolved sampling using an aerosol mass spectrometer (AMS) capable of single-particle measurements (details below) deployed on a mobile laboratory (a gasoline-powered cargo van). Sampling was performed while driving the laboratory through various neighborhoods in the Pittsburgh region. The mobile laboratory contained other on-line instruments including a NanoScan particle sizer (TSI Inc.) and gas monitors. The sampling inlets were mounted on the roof of the mobile lab and there was negligible self-sampling. When the van was stationary with the engine on, we observed no increase of signals measured by the onboard instruments. When the van was moving, self-sampling was even less likely because of the inlet location. More detailed information about the mobile laboratory can be found in Li et al. (2016).

We conducted systematic sampling in areas having large contrasts in traffic and restaurant emissions. We drove the van in 20 neighborhoods (Figure 2) covering upwind suburban, city center, and downwind suburban areas with different land-use types. Each neighborhood was visited one to six times. We visited a neighborhood only once within a sampling day and we sampled only during weekdays free of precipitation. We also conducted our measurements in different hours of the day (rush hour, nonrush hour, mealtime, non-mealtime) to reduce biases toward low or high emissions. In each visit, we endeavored to cover all streets in the neighborhood, which took 30–60 min. In total, we analyzed about 92,000 individual particles collected during the mobile sampling.

In addition to mobile sampling, we also collected stationary data when the mobile lab returned from the field and was parked at the Carnegie Mellon University (CMU) campus, which represents an urban background location without significant local emissions. The CMU campus is used as a central reference site in this study. We also performed continuous stationary sampling at the CMU campus using a scanning mobility particle sizer (SMPS; TSI Inc.) to measure particle number size distribution. Data from the SMPS were used for temporal corrections (described in the next section, "Source-Resolved Particle Number Measurements from Single-Particle Mass Spectrometry") of the mobile sampling data.

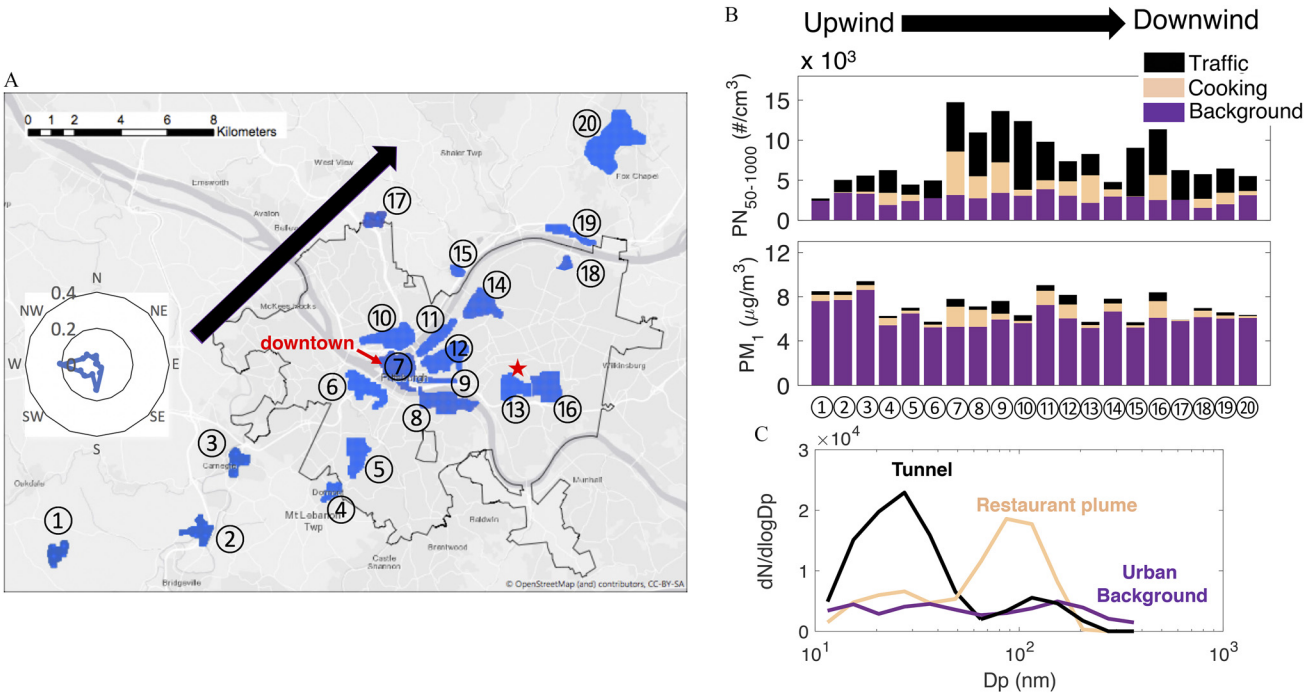

Figure 2. (A) A map showing the 20 neighborhoods (filled areas) where we made spatially resolved measurements of individual particle concentration and chemical composition as well as the central reference site (CMU campus, red star). The black arrow shows the prevailing winds in Pittsburgh with an inset showing the distribution of wind direction (hourly wind data from https://www.wunderground.com). (B) Number concentration (from this study) and mass concentration (from Gu et al. 2018) for the 20 areas ordered from upwind to downwind locations. The number concentration shows a larger spatial variability across the urban area compared with particle mass. It is mainly driven by primary emissions from traffic and cooking. The mass concentration is dominated by background particles and shows much smaller spatial variability. (C) Size distribution for three representative environments measured by a NanoScan particle sizer (TSI Inc.) on a mobile van: in a tunnel, in a restaurant plume, and at the CMU campus urban background site. The upper tail of the distribution in the tunnel is from background air that gets pulled into the tunnel. Note: CMU, Carnegie Mellon University campus; dN, particle number; D_p, particle diameter; PM_1, mass concentration of particulate matter with a diameter less than 1 micrometer; $PN_{50–1000}$, number concentration of particulate matter with a diameter between 50 and 1,000 nm.

Source-Resolved Particle Number Measurements from Single-Particle Mass Spectrometry

The central instrument is an AMS (Aerodyne Research, Inc.) that can measure both aggregated particle mass as well as single-particle size and composition. The bulk particle mass data are described by Gu et al. (2018). The single-particle mode in the AMS can obtain quantitative mass spectral signals as well as the aerodynamic diameter for each individual particle detected. A detailed description of the single-particle mass spectrometer can be found in the Supplemental Material in "Single particle aerosol mass spectrometer" and in Ye et al. (2018) and Onasch et al. (2012). The AMS used in our study can measure nonrefractory components (organics, sulfate, ammonium, nitrate, and chloride) but also black carbon soot in particles. In the AMS, vaporization and ionization processes are separated, producing consistent mass spectra for particles consisting of similar chemical species. The electron ionization (EI) fragments individual organic molecules (into a mass spectrum) so the AMS does not provide molecular speciation but, rather, quantifies the aggregate organic composition (C, H, O, N) within an individual particle. This allows us to identify sources of particles based on the well-documented mass fragments (Allan et al. 2004) and their spectral similarity to particles from known sources summarized in the AMS spectral database (http://cires1.colorado.edu/jimenez-group/AMSsd/).

For the thousands of individual particles collected in every neighborhood, we first performed *k*-means clustering on their normalized mass spectra, separating the particles into a number of distinguishable groups. Then, by comparing the average mass spectrum of each group to the AMS database, we identified the source of each group. Broadly, particles are categorized into three types, two types of freshly emitted particles and background particles. First are what we refer to as traffic particles in the remainder of this paper: hydrocarbon organic aerosol (HOA) particles that are rich in reduced organic fragments (e.g., $C_nH_{2n+1}^+$) and may contain soot fragments (e.g., C_3^+). They are associated with vehicular emissions (Zhang et al. 2011). Second are cooking organic particles (COA) that are rich in $C_mH_{2m-1}CO^+$ and are associated with cooking emissions (Zhang et al. 2011). We refer to them as cooking particles. Third are background particles that contain a dominant fraction of inorganic species such as sulfate or nitrate, and/or oxygenated organic fragments (e.g., COO^+ and $C_2H_3O^+$) (Zhang et al. 2005). These secondary fragments indicate that these particles have undergone considerable atmospheric aging. We show the average mass spectrum of each group in Figure S1 with comparisons with known sources in Figure S2. Each particle is categorized into only one group. However, in reality, an individual particle may contain more than one chemical fingerprint, for example, a particle may contain both reduced organics and sulfate. The grouping and source attribution are based on the dominant chemical fingerprints.

Due to the design of the AMS inlet, we only collected particles from 50–1,000 nm in aerodynamic diameter (D_p). Single-particle detection is based on the ion signals generated by individual particles and the detection is triggered only when the signals exceed a user-defined threshold. The single-particle AMS detects only a fraction of the particles sampled into the instrument due to the instrument dead time and the insufficient signals generated by some of the particles. Smaller particles have lower detection efficiency because they generate fewer ions. To quantify particle number concentration measured from the single-particle AMS, we performed size-dependent corrections on the particle number measured by the AMS using the number measured from the SMPS when the van was parked on campus. The SMPS was operated continuously throughout the entire campaign in the central reference site. The correction factors are the ratios of number concentrations measured by the SMPS and the number concentrations measured by the AMS in different size bins (Qin et al. 2006), as shown in Figure S3. The uncertainty (relative standard deviation) of the correction factor was estimated to be 15–46% (shown as error bars in Figure S3) depending on particle size and instrument stability on a day-to-day basis.

We also used particle number measurements from the SMPS to adjust for temporal variations of our mobile sampling. The adjustment factors were computed using N_t/N_{avg}, the ratio of number concentration during the time of the sampling and the annual average number concentration derived from the SMPS. The AMS does not detect road dust, one important type of PM in the urban environment (Rogge et al. 1993). However, we did not expect road dust to be a major source for particle number (or mass) <1,000 nm.

Particle Mixing State Quantification

To quantify the chemical mixing state of a particle population, we used the mixing state metric χ based on information–theoretic entropy measures developed by Riemer and West (2013). χ quantifies the diversity of chemical species in individual particles with respect to the whole particle population.

For a population of N particles, the mixing entropy value, H_i, for every particle is calculated as follows:

$$H_i = \sum_{a=1}^{A} - p_i^a \ln p_i^a.$$

The mass fraction of particle i in the particle population is p_i. A is the total number of chemical species. The mass fraction of chemical species a in the particle population is p^a. The mass fraction of species a in particle i is p_i^a. The average particle mixing entropy, H_α, is calculated using

$$H_\alpha = \sum_{i=1}^{N} p_i H_i.$$

The mixing entropy of the population is given by

$$H_\gamma = \sum_{a=1}^{A} - p^a \ln p^a.$$

The average single particle diversity (D_α) is

$$D_\alpha = e^{Ha},$$

and the bulk population diversity (D_γ) is

$$D_\gamma = e^{H\gamma}.$$

The mixing state metric χ is then calculated as

$$\chi = \frac{D_\alpha - 1}{D_\gamma - 1}.$$

Here we include organics, nitrate, sulfate, chloride, and black carbon in the mixing-state calculation. We do not include ammonium due to the large background interference in the instrument. We treat all organics as one chemical species, without further separation of fresh and aged organics. This is because of the small number of ions derived from individual particles, which precludes further separation on a single-particle basis.

For atmospheric particles, χ of a particle population is somewhere between 0% and 100%. Zero percent indicates full external mixing, meaning that the particle population consists of individual

particles with distinct chemical constituents. One hundred percent indicates full internal mixing, meaning all particles have identical composition. χ in the urban background areas of Pittsburgh and of Paris, France, are found to be 50–60%, suggesting particles are midway between a complete external and a complete internal mixture (Healy et al. 2014; Ye et al. 2018).

Land-Use Regression Models

To predict the fine spatial-scale number concentration (in n/cm^3) of traffic and cooking particles as well as the chemical mixing state of particle populations in Pittsburgh, we built LUR models using available land-use predictors with a range of buffer areas. We first constructed raster cells at 5 m × 5 m resolution using ArcGIS (Esri). Each raster has the associated land-use values. For any grid sizes that we used to build the models (for sampling neighborhoods or the subdivided areas, see below), we used the ArcGIS tool zonal statistics to calculate corresponding land-use values based on the 5 m × 5 m raster cells. We list all of the covariates and the data sources in Table S1. These data are from the databases of the Allegheny County Health Department (http://infoportal.alleghenycounty.us/data.html), the Pennsylvania Department of Transportation, the National Emission Inventory (https://www.epa.gov/air-emissions-inventories/2017-national-emissions-inventory-nei-data), the Pennsylvania Spatial Data Access (http://www.pasda.psu.edu/uci/DataSummary.aspx?dataset=56), and the U.S. Census (https://www.census.gov/geographies/reference-maps/2010/geo/2010-census-tract-maps.html).

We used a similar model construction procedure as used by Li et al. (2016) and Eeftens et al. (2012). In brief, we used the forward variable selection approach to select the covariates, which only added a new covariate to the model if it produced the highest R^2. The variable selection process continued until the newly added covariates improved the overall R^2 by <0.01. For all of the covariates selected, we further examined their p-values and removed those having $p > 0.1$. Last, we tested the variance inflation factors (VIF) for collinearity and removed covariates with VIF >3.

We derived separate models to predict three quantities: *a*) number concentration of traffic particles, *b*) number concentration of cooking particles, and *c*) particle mixing state. For traffic and cooking particle concentration predictions, because our measurements are source-resolved, we restricted the models to select only covariates from categories related to vehicle emissions and cooking activities. These categories include traffic, restaurants, housing, population, commercial land use, and elevation. We refer to these models as source-specific LUR models. For comparison, we also developed models for traffic and cooking particles using covariates from all land-use categories, which we refer to as full LUR models. The two types of LUR models agreed well, as shown in "Results" section. For mixing state prediction, given that we did not have prior knowledge about what categories of covariates may affect mixing state, we developed a full LUR model using all covariates.

As described above and in Figure 2, we sampled 20 neighborhoods in Pittsburgh and its surrounding regions. Our final LUR models were built using 200 m × 200 m spatial resolution. Ideally, we would subdivide all neighborhoods into 200 m × 200 m areas for model construction. However, we did not have enough collected particles to do so. We were only able to subdivide 10 of the 20 neighborhoods into 200 m × 200 m grids (see Figure S4). There were two reasons. First, there was sufficient signal for us to further subdivide the 10 more urban neighborhoods that had higher particle concentrations. The other 10 neighborhoods were more suburban/rural, so we collected comparatively fewer particles. Second, as shown in Figure S5, the 10 subdivided areas had large subneighborhood variabilities in vehicle and restaurant density, two main sources for ambient particles we identified. The other 10 neighborhoods were relatively homogenous in vehicle and restaurant density and were therefore expected to be more homogeneous in terms of pollutant concentrations (Li et al. 2019).

We used the neighborhoods and the subdivided 200 m × 200 m areas that had 250 or more detected particles to build the LUR models. We established this criterion by first calculating the normalized size distribution from the particles collected at the CMU campus, then deriving the normalized size distribution from particles randomly sampled from the particle pool. By looking at the estimated errors of size distributions from the subsamples as a function of the sample size, we determined that a sample size of 250 particles was sufficient to reproduce the size distribution of the entire population with relatively small errors (see Figure S6). There were fifty-five 200 m × 200 m small areas with more than 250 detected particles. Combining the remaining 10 neighborhoods, we used 65 distinct areas to build the models. In total, we had about 250 area-visits that covered about 14 km^2, shown in Figure S4. We also developed models using only the 200 m × 200 m subdivided areas. As discussed in the "Results" section, two types of models shared highly similar predictors.

We evaluated LUR model performance using R^2, 10-fold cross validation, absolute mean error (AME), and root mean square error (RMSE). For the cross validation, we randomly partitioned the measurement data into 10 equal-sized subgroups. Every time, we used 1 subgroup as the validation data to test the model and 9 subgroups as training data. We repeated the process so that every subgroup was used once as the validation data set.

Results

Freshly Emitted Particle Number Drives Spatial Variability Invisible in Mass

Figure 2A is a map showing the 20 mobile sampling neighborhoods and the CMU campus site. We numbered the neighborhoods from upwind to downwind. Figure 2B contrasts the number with mass concentration for the sampling areas along the prevailing wind direction. There is a large spatial heterogeneity of total number concentration across the urban scale. This heterogeneity is mostly driven by freshly emitted particles, whereas the concentration of background particles is relatively homogeneous spatially. In areas upwind of the city, the majority of the particles are aged background particles that are presumably transported regionally and have experienced extensive atmospheric processing. As air masses travel to the city center, the concentrations of freshly emitted particles grow substantially due to emissions from traffic and restaurant cooking. In these areas, the freshly emitted particle number concentration exceeds the background particle number concentration by more than a factor of three in the size range of 50–1,000 nm measured by our instrument. In downwind suburban areas such as neighborhood 20, which has low vehicle and restaurant activity, freshly emitted particle number concentrations are greatly reduced, similar to upwind background locations. This indicates that emission intensity is the main driving force for the spatial complexity of particle number concentration across the urban scale in our study.

In contrast, particle mass concentration shows much less spatial variability than particle number. Aged background particles dominate total mass in all areas across the city. The modest variability of background particle mass is likely due to imperfect temporal corrections and uncertainties in the instrument. Traffic and cooking particle mass increase in the city center but only contribute about 10% to the total mass concentration.

Figure 2C shows the size distribution of three particle types measured by the NanoScan particle sizer (11.5–365 nm size range). The NanoScan does not resolve particle source information

Table 1. Summary of source-specific LUR models for traffic and cooking particle number concentration and mixing state in Pittsburgh, Pennsylvania.

Covariates selected[a]	Coefficient	Partial R^2	Model R^2	Ten-fold validation R^2	RMSE (n/cm^3)	AME (n/cm^3)
Traffic	—	—	0.58	0.54	1,936	1,524
Vehicle density in all roads (100 m)	21.48	0.37	—	—	—	—
Diesel annual average daily travel × squared inverse distance to the nearest road (100 m)	321.5	0.21	—	—	—	—
Intercept	1,577	—	—	—	—	—
Cooking	—	—	0.67	0.61	1,479	1,119
Restaurant counts (100 m)	12.87	0.37	—	—	—	—
Major road length (1,000 m)	0.0505	0.24	—	—	—	—
Population density (1,000 m)	0.1633	0.06	—	—	—	—
Intercept	−717.8	—	—	—	—	—
Mixing State ($1-\chi$), unitless	—	—	0.63	0.58	0.06	0.05
Major road length (1,000 m)	5.77×10^{-6}	0.54	—	—	—	—
House density (300 m)	7.59×10^{-5}	0.06	—	—	—	—
NEI point source density (30 km)	9.44	0.03	—	—	—	—
Intercept	−0.304	—	—	—	—	—

Note: —, not applicable; AME, absolute mean error; LUR, land-use regression; NEI, National Emission Inventory; RMSE, root mean square error.
[a]Covariate data sources: Allegheny County Health Department (http://infoportal.alleghenycounty.us/data.html), Pennsylvania Department of Transportation, National Emission Inventory (https://www.epa.gov/air-emissions-inventories/2017-national-emissions-inventory-nei-data), Pennsylvania Spatial Data Access (http://www.pasda.psu.edu/uci/DataSummary.aspx?dataset=56), U.S. Census (https://www.census.gov/geographies/reference-maps/2010/geo/2010-census-tract-maps.html).

but because we sampled in representative source-dominated locations (inside a tunnel and inside a restaurant plume), we are confident that the sources of fresh emissions were almost exclusively traffic and restaurant cooking, respectively. As Figure 2C shows, the size distribution of traffic particles has the smallest mode. Total particle number concentration is also highest in the traffic tunnel, illustrating the high emissions of particle number from vehicles. Cooking particles are larger than fresh traffic emissions, and aged background particles, which have grown by coagulation and condensation, are the largest. This explains why, though they are more numerous in the source-active areas and the primary driver for intra-city variations in particle number, traffic and cooking particles contribute (much) less to particle mass than background particles (Figure 2B).

Model Predictions of Sourced-Resolved Particle Number and Mixing State

As described in the "Methods" section, we built LUR models to predict the spatial distribution of traffic and cooking particle number concentrations as well as particle mixing state. Table 1 summarizes the selected covariates, validation, and performance of the models. Vehicle density, restaurant counts, and major road length are the major covariates selected to predict traffic particles, cooking particles, and mixing state, respectively.

Predicted number concentrations of traffic and cooking particles in the Pittsburgh area using source-specific LUR models are shown in Figure 3A,B. Overall, concentrations are highest in the downtown (Area 7 in Figure 2). This neighborhood had the highest density of both traffic and restaurants in our sampling domain. The spatial pattern of traffic particles followed the road network. Traffic particle concentrations varied by more than one order of magnitude across the city. The concentration of cooking particles also shows large intra-city spatial heterogeneity with several clusters of hotspots in locations with high restaurant density. The AMS only detects particles ranging from 50–1,000 nm. We expect that if we had included particles <50 nm, the spatial variability of freshly emitted particle number concentrations would have been even larger.

The full LUR models yielded similar patterns as the source-specific LURs for cooking and traffic particles. Table S2 and Figures S7 and S8 show these models. The full LUR models select similar covariates to the source-specific models. For both cooking and traffic, the strongest predictor is the same in both the full and source-specific LURs. This illustrates the strong connection between emission sources and source-resolved particles measured here.

Figure 3C shows the predicted spatial distribution of particle mixing state. In general, particle populations in the downtown and other areas with high fresh emissions were predicted to be more externally mixed, whereas particles in suburban areas low in source activities were more internally mixed. The mixing state metric χ varies by more than a factor of two across the sampling domain.

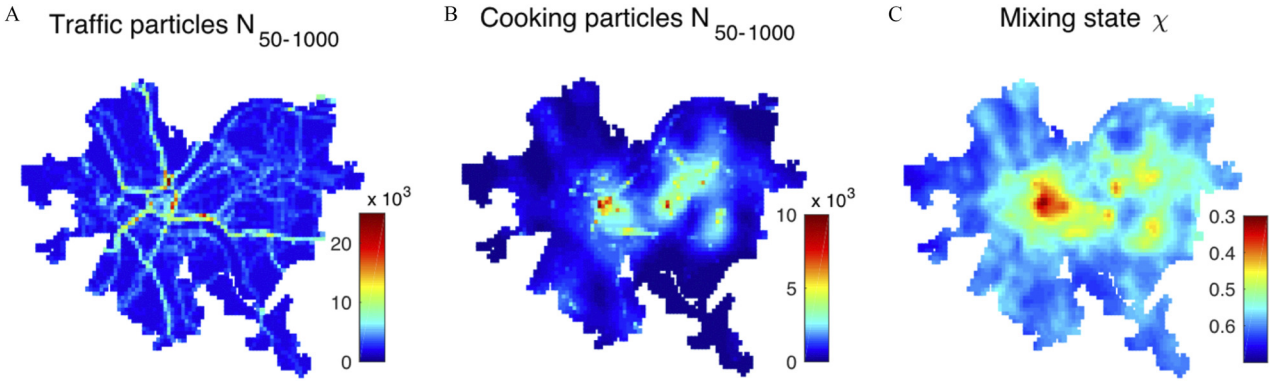

Figure 3. Predicted number concentration (n/cm^3) of (A) traffic particles, (B) cooking particles and (C) mixing state index (χ, unitless) in Pittsburgh, Pennsylvania. Hot colors (red) indicate high number concentrations and a low (more externally mixed) mixing-state index. Spatial resolution is 200 m × 200 m. Note: $N_{50-1000}$, number of particles from 50–1,000 nm in aerodynamic diameter (D_p).

As described above, our LUR models were built from a combination of 200 m × 200 m areas and larger neighborhoods. We tested the sensitivity of our models to this choice of aggregation. Table S3 shows source-specific LUR models built only from the 200 m × 200 m areas. Overall, these LURs used the same covariates as the source-specific (Table 1) and full (see Table S2) LURs that used all of the available data for model building, though model R^2 values were slightly lower.

Source-Resolved Particle Number and Mixing State Exposure

We combined our predictions of source-resolved particle concentrations with American Community Survey U.S. Census block group data (https://www.census.gov/geo/maps-data/) to calculate the fine-scale population exposure in every grid cell of the domain (200-m resolution). We then aggregated the results to characterize the cumulative population exposure. Figure 4A shows the cumulative population exposure to particle number concentration. It also incorporates the corresponding particle mixing state in each grid cell, shown as color coding along the edge of the total particle number concentration. We contrast this new picture of population exposure with source-resolved particle-mass-based concentration for Pittsburgh using data from Gu et al. (2018), which deconvolved particle mass to the same sources and had the same spatial resolution, shown in Figure 4B. Figure 4B is analogous to conventional bulk mass-based measurements.

As Figure 4 shows, background particles contribute to both particle mass and number concentrations. Here we used the median concentration measured at the CMU campus, an urban background site because background particles were spatially homogenous (Figure 2). Background particles contribute the majority of particle mass but are a much less important contributor to particle number. For example, Figure 4 indicates that more than 80% of the population is exposed to a total number concentration more than twice the background level. In contrast, due to the small mass contribution of freshly emitted particles, the overall spatial variability of mass exposure was relatively small—more than 80% of the population was exposed to concentrations of freshly emitted particles that were within 20% of the background mass concentration.

Figure 4A also shows that particle number concentration correlates with particle mixing state. People who are exposed to elevated particle number concentrations are also exposed to a more externally mixed particle population. Again, this information cannot be resolved using conventional methods purely based on particle mass.

Figure 4 shows that traffic and cooking have different contributions to particle mass and number exposures. As shown in Figure 4B and described by Gu et al. (2018), fresh cooking emissions have an equal or larger contribution to particle mass exposures than fresh traffic emissions. However, Figure 4A shows that traffic was a larger contributor to particle number exposures. This is also apparent in Figure 3, where the predicted range of traffic particle concentrations is more than double the range for cooking particles. This occurred because vehicles have high emissions of small particles (Figure 2C) that contribute more to particle number than to mass.

We also compared the particle number concentration of traffic and cooking particles in different communities stratified by race and household income (see Figure S9). We found no significant trend of exposure injustice for traffic particles in Pittsburgh. We attribute this to the fact that in Pittsburgh most minority and low-income neighborhoods do not contain major highways or arterial roads. Other U.S. cities may have different spatial patterns. Asians are predicted to be exposed to a higher level of cooking particles than other races. This could be due to the fact that neighborhoods containing the two major university campuses in Pittsburgh where many Asian students live also have high restaurant densities.

Discussion

A More Realistic Estimate of Fine Particle Exposure

By using advanced single-particle mass spectrometry that resolves detailed physiochemical information of atmospheric particles, we provide a more atmospherically realistic picture of spatial distribution of fine particle concentrations in a populous urban environment. Our new perspective much more closely matches the state of

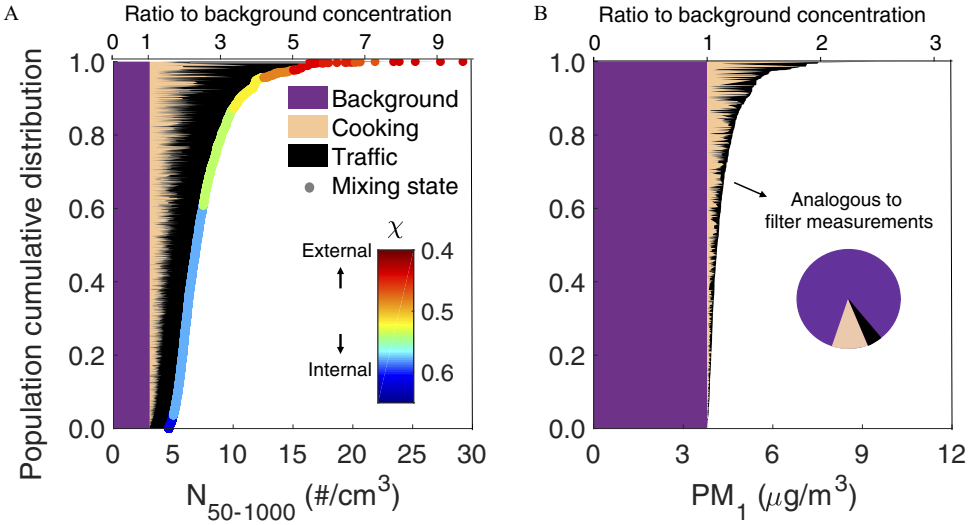

Figure 4. Normalized cumulative distribution of population exposure to background, traffic particles, and cooking particles on a (A) particle number concentration and a (B) particle mass concentration basis. Results are based on predictions of the source-resolved LUR models in Pittsburgh. The curve of total particle number in A is color-coded by the particle chemical mixing state. The background particle number concentration is the median concentration measured at the CMU campus, the central site of this campaign. Particle mass data in B are from Gu et al. (2018). Note: CMU, Carnegie Mellon University campus; LUR, land-use regression.

PM as it actually exists in the atmosphere (and what we breathe) compared with bulk measurements.

Considering particle number versus mass substantially alters our perspectives on population exposure to fine PM. Our results suggest that within-city variability of PM pollution is much larger than conventional mass-based methods indicate. Therefore, our results significantly extend many existing intra-city particle exposure estimates, which are based solely on mass (Eeftens et al. 2012; Henderson et al. 2007; Just et al. 2015; Moore et al. 2009), by showing much larger spatial gradients of source-resolved particle number concentration compared with source-resolved mass concentration.

Appropriately resolving the patterns of freshly emitted particle pollution is important for understanding spatial variations of PM exposure and intra-city variations of PM health effects. First, our results highlight that freshly emitted and background particles differ significantly in size, which determines their deposition efficiency in the respiratory tract. Second, our results demonstrate that freshly emitted and background particles have distinct chemical composition important to toxicities. Fresh emissions are generally more hydrophobic than aged background particles, which are dominated by oxidized organics and sulfate (see Figure S1). Fresh traffic particles also contain black carbon and particle-bound metals (the latter of which were not detected in our measurements). Third, freshly emitted particles are often strongly associated/co-emitted with other primary hazardous pollutants such as carbon monoxide and nitrogen oxides (Brown et al. 2012; Lanz et al. 2007), which has strong implications for multipollutant health effects (Dominici et al. 2010).

A growing body of research demonstrates that intra-urban air pollution exposure gradients may lead to risk contrasts at least as large as those that result from differences in urban background concentrations among individual cities, and related work has suggested that certain source-related air pollution signatures may have enhanced health risks (Jerrett et al. 2005; Thurston et al. 2016). Alexeeff et al. (2018) showed that intra-urban differences in source-related exposure—in their case, exposure to traffic air pollutants—contributed to fine-scale differences in cardiovascular health within individual neighborhoods. Our chemical measurements of individual particles with mobile sampling more directly resolve the source-related particle number at finer spatial scale compared with studies that relied on statistical methods and stationary measurements (Kim et al. 2004; Sowlat et al. 2016; Squizzato et al. 2019). Future studies incorporating these types of measurements can assist in improving the assessments of health burden attributable to different sources and ultimately facilitate effective pollution control.

Our detailed measurements of the chemical composition of individual particles by single-particle mass spectrometry also allow us to determine the chemical mixing state of the particle populations we sampled. This, to our knowledge, is the first study that evaluates the spatial variation in mixing state and its effects on population exposure. Our results indicate that external mixing is associated with a high number concentration. Health effects of chemical mixing state are largely unexplored and therefore uncertain, but some studies have revealed a potential health influence of particle mixing state (Ching et al. 2019; Ching and Kajino 2018).

The overall approach we developed in this study serves as a good starting point to characterize intra-urban PM exposure beyond mass in other cities. The particle number concentration and chemical mixing state in Pittsburgh are strongly associated with common sources in urban environments. Future studies can apply a similar approach to other major metropolitan areas to examine transferability and generalizability of this approach and ultimately refine PM exposure estimates on the national scale.

Limitations

The number concentrations and mixing state values we predict here are from relatively short-term sampling because we visited each neighborhood a limited number of times (one to six times). Many LUR models for predicting ultrafine particle concentration are based on short-term mobile or stationary sampling (Saha et al. 2019) and increasing sampling time will improve model performance. As mentioned above, for areas we sampled multiple times, our visits were spread out over different times of the day to reduce biases toward low or high emission scenarios. PM pollution from fresh emissions such as traffic and cooking activities can have strong temporal profiles in Pittsburgh (Robinson et al. 2018); background particle concentrations are also temporally variable. The major source areas of fresh emissions—roads and restaurants—are stationary, therefore spatial patterns of source-resolved PM should be relatively robust (e.g., downtown should always have more traffic particles than the urban background). Given the size of our current data set, we were not able to resolve temporal variations but, rather, present a picture of average concentrations. Future studies should increase the sampling time for better temporal resolution. In addition, the different frequency of visits to each neighborhood may cause some uncertainties in the spatial patterns of model inputs. However, several other studies from the same campaign that conducted a greater number of visits to the neighborhoods have identified similar sources and spatial variations of source-specific pollutant level in Pittsburgh (Gu et al. 2018; Li et al. 2019; Robinson et al. 2018). This indicates that the spatial patterns of our model inputs should be relatively robust.

The detection efficiency of particles decreases as particle size decreases in our instrument, causing higher uncertainties for quantifying the concentration of small particles. In addition, our analysis does not include nucleation as a source for ultrafine particles due to the size cutoff of the AMS measurements. Nucleation in Pittsburgh is likely a minor contributor to particle number concentration at present. A recent study by Saha et al. (2018) showed that the frequency and intensity of nucleation in Pittsburgh has been reduced by half over the past 15 y and that locally nucleated particles constitute only around 6% of the particle number concentration. We also did not quantify particulate metal measurements because metal quantification by the instrument is challenging (Carbone et al. 2015). Regardless, this work is, to our knowledge, the first to measure and predict both source-resolved number concentration and particle chemical mixing state of ambient PM, providing a more atmospherically realistic exposure estimate.

Acknowledgments

We sincerely thank J. Marshall at the University of Washington for insightful discussions. This work was part of the Center for Air, Climate, and Energy Solutions (CACES), which was supported under assistance agreement no. RD83587301 awarded by the U.S. Environmental Protection Agency (EPA). It has not been formally reviewed by the U.S. EPA. The views expressed in this document are solely those of the authors and do not necessarily reflect those of the agency. The U.S. EPA does not endorse any products or commercial services mentioned in this publication. This work was also supported by the U.S. National Science Foundation under grants ATM-1543786, MRI-CBET0922643, and CHE-1412309. Q.Y. also thanks the support from the Faculty for the Future Fellowship from the Schlumberger Foundation.

References

Alexeeff SE, Roy A, Shan J, Liu X, Messier K, Apte JS, et al. 2018. High-resolution mapping of traffic related air pollution with Google street view cars and incidence of cardiovascular events within neighborhoods in Oakland, CA. Environ Health 17(1):38, PMID: 29759065, https://doi.org/10.1186/s12940-018-0382-1.

Allan JD, Delia AE, Coe H, Bower KN, Alfarra MR, Jimenez JL, et al. 2004. Technical note: a generalised method for the extraction of chemically resolved mass spectra from Aerodyne aerosol mass spectrometer data. J Aerosol Sci 35(7):909–922, https://doi.org/10.1016/j.jaerosci.2004.02.007.

Baldauf RW, Devlin RB, Gehr P, Giannelli R, Hassett-Sipple B, Jung H, et al. 2016. Ultrafine particle metrics and research considerations: review of the 2015 UFP workshop. Int J Environ Res Public Health 13(11):E1054, PMID: 27801854, https://doi.org/10.3390/ijerph13111054.

Brown SG, Lee T, Norris GA, Roberts PT, Collett JL Jr, Paatero P, et al. 2012. Receptor modeling of near-roadway aerosol mass spectrometer data in Las Vegas, Nevada, with EPA PMF. Atmos Chem Phys 12(1):309–325, https://doi.org/10.5194/acp-12-309-2012.

Carbone S, Onasch T, Saarikoski S, Timonen H, Saarnio K, Sueper D, et al. 2015. Characterization of trace metals on soot aerosol particles with the SP-AMS: detection and quantification. Atmos Meas Tech 8(11):4803–4815, https://doi.org/10.5194/amt-8-4803-2015.

Cassee FR, Héroux ME, Gerlofs-Nijland ME, Kelly FJ. 2013. Particulate matter beyond mass: recent health evidence on the role of fractions, chemical constituents and sources of emission. Inhal Toxicol 25(14):802–812, PMID: 24304307, https://doi.org/10.3109/08958378.2013.850127.

Ching J, Adachi K, Zaizen Y, Igarashi Y, Kajino M. 2019. Aerosol mixing state revealed by transmission electron microscopy pertaining to cloud formation and human airway deposition. NPJ Clim Atmos Sci 2(1):22, https://doi.org/10.1038/s41612-019-0081-9.

Ching J, Kajino M. 2018. Aerosol mixing state matters for particles deposition in human respiratory system. Sci Rep 8(1):8864, PMID: 29891990, https://doi.org/10.1038/s41598-018-27156-z.

Cross ES, Slowik JG, Davidovits P, Allan JD, Worsnop DR, Jayne JT, et al. 2007. Laboratory and ambient particle density determinations using light scattering in conjunction with aerosol mass spectrometry. Aerosol Sci Technol 41(4):343–359, https://doi.org/10.1080/02786820701199736.

Dominici F, Peng RD, Barr CD, Bell ML. 2010. Protecting human health from air pollution: shifting from a single-pollutant to a multipollutant approach. Epidemiology 21(2):187–194, PMID: 20160561, https://doi.org/10.1097/EDE.0b013e3181cc86e8.

Downward GS, Van Nunen E, Kerckhoffs J, Vineis P, Brunekreef B, Boer JMA, et al. 2018. Long-term exposure to ultrafine particles and incidence of cardiovascular and cerebrovascular disease in a prospective study of a Dutch cohort. Environ Health Perspect 126(12):127007, PMID: 30566375, https://doi.org/10.1289/EHP3047.

Eeftens M, Beelen R, de Hoogh K, Bellander T, Cesaroni G, Cirach M, et al. 2012. Development of land use regression models for $PM_{2.5}$, $PM_{2.5}$ absorbance, PM_{10} and PM_{coarse} in 20 European study areas; results of the ESCAPE project. Environ Sci Technol 46(20):11195–11205, PMID: 22963366, https://doi.org/10.1021/es301948k.

Franklin M, Zeka A, Schwartz J. 2007. Association between $PM_{2.5}$ and all-cause and specific-cause mortality in 27 US communities. J Expo Sci Environ Epidemiol 17(3):279–287, PMID: 17006435, https://doi.org/10.1038/sj.jes.7500530.

Freedman MA, Ott E-JE, Marak KE. 2019. The role of pH in aerosol processes and measurement challenges. J Phys Chem A 123(7):1275–1284, PMID: 30586311, https://doi.org/10.1021/acs.jpca.8b10676.

Fuzzi S, Baltensperger U, Carslaw K, Decesari S, Denier Van Der Gon H, Facchini MC, et al. 2015. Particulate matter, air quality and climate: lessons learned and future needs. Atmos Chem Phys 15(14):8217–8299, https://doi.org/10.5194/acp-15-8217-2015.

Gu P, Li HZ, Ye Q, Robinson ES, Apte JS, Robinson AL, et al. 2018. Intra-city variability of particulate matter exposure is driven by carbonaceous sources and correlated with land use variables. Environ Sci Technol 52(20):11545–11554, PMID: 30248264, https://doi.org/10.1021/acs.est.8b03833.

Hamra GB, Guha N, Cohen A, Laden F, Raaschou-Nielsen O, Samet JM, et al. 2014. Outdoor particulate matter exposure and lung cancer: a systematic review and meta-analysis. Environ Health Perspect 122(9):906–911, PMID: 24911630, https://doi.org/10.1289/ehp/1408092.

Healy RM, Riemer N, Wenger JC, Murphy M, West M, Poulain L, et al. 2014. Single particle diversity and mixing state measurements. Atmos Chem Phys 14(12):6289–6299, https://doi.org/10.5194/acp-14-6289-2014.

Henderson SB, Beckerman B, Jerrett M, Brauer M. 2007. Application of land use regression to estimate long-term concentrations of traffic-related nitrogen oxides and fine particulate matter. Environ Sci Technol 41(7):2422–2428, PMID: 17438795, https://doi.org/10.1021/es0606780.

Herner JD, Green PG, Kleeman MJ. 2006. Measuring the trace elemental composition of size-resolved airborne particles. Environ Sci Technol 40(6):1925–1933, PMID: 16570617, https://doi.org/10.1021/es052315q.

Highwood EJ, Kinnersley RP. 2006. When smoke gets in our eyes: the multiple impacts of atmospheric black carbon on climate, air quality and health. Environ Int 32(4):560–566, PMID: 16513170, https://doi.org/10.1016/j.envint.2005.12.003.

Hoek G, Beelen R, de Hoogh K, Vienneau D, Gulliver J, Fischer P, et al. 2008. A review of land-use regression models to assess spatial variation of outdoor air pollution. Atmos Environ 42(33):7561–7578, https://doi.org/10.1016/j.atmosenv.2008.05.057.

Jerrett M, Burnett RT, Ma R, Pope CA III, Krewski D, Newbold KB, et al. 2005. Spatial analysis of air pollution and mortality in Los Angeles. Epidemiology 16(6):727–736, PMID: 16222161, https://doi.org/10.1097/01.ede.0000181630.15826.7d.

Just AC, Wright RO, Schwartz J, Coull BA, Baccarelli AA, Tellez-Rojo MM, et al. 2015. Using high-resolution satellite aerosol optical depth to estimate daily $PM_{2.5}$ geographical distribution in Mexico City. Environ Sci Technol 49(14):8576–8584, PMID: 26061488, https://doi.org/10.1021/acs.est.5b00859.

Kerckhoffs J, Hoek G, Messier KP, Brunekreef B, Meliefste K, Klompmaker JO, et al. 2016. Comparison of ultrafine particle and black carbon concentration predictions from a mobile and short-term stationary land-use regression model. Environ Sci Technol 50(23):12894–12902, PMID: 27809494, https://doi.org/10.1021/acs.est.6b03476.

Kim E, Hopke PK, Larson TV, Covert DS. 2004. Analysis of ambient particle size distributions using Unmix and positive matrix factorization. Environ Sci Technol 38(1):202–209, PMID: 14740737, https://doi.org/10.1021/es030310s.

Landis MS, Norris GA, Williams RW, Weinstein JP. 2001. Personal exposures to $PM_{2.5}$ mass and trace elements in Baltimore, MD, USA. Atmos Environ 35(36):6511–6524, https://doi.org/10.1016/S1352-2310(01)00407-1.

Lanz VA, Alfarra MR, Baltensperger U, Buchmann B, Hueglin C, Prévôt ASH. 2007. Source apportionment of submicron organic aerosols at an urban site by factor analytical modelling of aerosol mass spectra. Atmos Chem Phys 7(6):1503–1522, https://doi.org/10.5194/acp-7-1503-2007.

Li HZ, Dallmann TR, Gu P, Presto AA. 2016. Application of mobile sampling to investigate spatial variation in fine particle composition. Atmos Environ 142:71–82, https://doi.org/10.1016/j.atmosenv.2016.07.042.

Li HZ, Gu P, Ye Q, Zimmerman N, Robinson ES, Subramanian R, et al. 2019. Spatially dense air pollutant sampling: implications of spatial variability on the representativeness of stationary air pollutant monitors. Atmos Environ X 2:100012, https://doi.org/10.1016/j.aeaoa.2019.100012.

Li X, Dallmann TR, May AA, Stanier CO, Grieshop AP, Lipsky EM, et al. 2018. Size distribution of vehicle emitted primary particles measured in a traffic tunnel. Atmos Environ 191:9–18, https://doi.org/10.1016/j.atmosenv.2018.07.052.

Miguel AH, Kirchstetter TW, Harley RA, Hering SV. 1998. On-road emissions of particulate polycyclic aromatic hydrocarbons and black carbon from gasoline and diesel vehicles. Environ Sci Technol 32(4):450–455, https://doi.org/10.1021/es970566w.

Moffet RC, de Foy B, Molina LT, Molina MJ, Prather KA. 2008. Measurement of ambient aerosols in northern Mexico City by single particle mass spectrometry. Atmos Chem Phys 8(16):4499–4516, https://doi.org/10.5194/acp-8-4499-2008.

Mohr C, Richter R, DeCarlo PF, Prévôt ASH, Baltensperger U. 2011. Spatial variation of chemical composition and sources of submicron aerosol in Zurich during wintertime using mobile aerosol mass spectrometer data. Atmos Chem Phys 11(15):7465–7482, https://doi.org/10.5194/acp-11-7465-2011.

Moore K, Krudysz M, Pakbin P, Hudda N, Sioutas C. 2009. Intra-community variability in total particle number concentrations in the San Pedro Harbor Area (Los Angeles, California). Aerosol Sci Technol 43(6):587–603, https://doi.org/10.1080/02786820902800900.

Onasch TB, Trimborn A, Fortner EC, Jayne JT, Kok GL, Williams LR, et al. 2012. Soot particle aerosol mass spectrometer: development, validation, and initial application. Aerosol Sci Technol 46(7):804–817, https://doi.org/10.1080/02786826.2012.663948.

Ostro B, Hu J, Goldberg D, Reynolds P, Hertz A, Bernstein L, et al. 2015. Associations of mortality with long-term exposures to fine and ultrafine particles, species and sources: results from the California Teachers Study Cohort. Environ Health Perspect 123(6):549–556, PMID: 25633926, https://doi.org/10.1289/ehp.1408565.

Patton AP, Zamore W, Naumova EN, Levy JI, Brugge D, Durant JL. 2015. Transferability and generalizability of regression models of ultrafine particles in urban neighborhoods in the Boston area. Environ Sci Technol 49(10):6051–6060, PMID: 25867675, https://doi.org/10.1021/es5061676.

Penttinen P, Timonen KL, Tiittanen P, Mirme A, Ruuskanen J, Pekkanen J. 2001. Number concentration and size of particles in urban air: effects on spirometric lung function in adult asthmatic subjects. Environ Health Perspect 109(4):319–323, PMID: 11335178, https://doi.org/10.1289/ehp.01109319.

Pope CA III, Dockery DW. 2006. Health effects of fine particulate air pollution: lines that connect. J Air Waste Manag Assoc 56(6):709–742, PMID: 16805397, https://doi.org/10.1080/10473289.2006.10464485.

Qin X, Bhave PV, Prather KA. 2006. Comparison of two methods for obtaining quantitative mass concentrations from aerosol time-of-flight mass spectrometry measurements. Anal Chem 78(17):6169–6178, PMID: 16944899, https://doi.org/10.1021/ac060395q.

Riemer N, West M. 2013. Quantifying aerosol mixing state with entropy and diversity measures. Atmos Chem Phys 13(22):11423–11439, https://doi.org/10.5194/acp-13-11423-2013.

Robinson AL, Donahue NM, Shrivastava MK, Weitkamp EA, Sage AM, Grieshop AP, et al. 2007. Rethinking organic aerosols: semivolatile emissions and photochemical aging. Science 315(5816):1259–1262, PMID: 17332409, https://doi.org/10.1126/science.1133061.

Robinson ES, Donahue NM, Ahern AT, Ye Q, Lipsky E. 2016. Single-particle measurements of phase partitioning between primary and secondary organic aerosols. Faraday Discuss 189:31–49, PMID: 27092377, https://doi.org/10.1039/c5fd00214a.

Robinson ES, Gu P, Ye Q, Li HZ, Shah RU, Apte JS, et al. 2018. Restaurant impacts on outdoor air quality: elevated organic aerosol mass from restaurant cooking with neighborhood-scale plume extents. Environ Sci Technol 52(16):9285–9294, PMID: 30070466, https://doi.org/10.1021/acs.est.8b02654.

Rogge WF, Hildemann LM, Mazurek MA, Cass GR, Simoneit BRT. 1993. Sources of fine organic aerosol. 3. Road dust, tire debris, and organometallic brake lining dust: roads as sources and sinks. Environ Sci Technol 27(9):1892–1904, https://doi.org/10.1021/es00046a019.

Saha PK, Li HZ, Apte JS, Robinson AL, Presto AA. 2019. Urban ultrafine particle exposure assessment with land-use regression: influence of sampling strategy. Environ Sci Technol 53(13):7326–7336, PMID: 31150214, https://doi.org/10.1021/acs.est.9b02086.

Saha PK, Robinson ES, Shah RU, Zimmerman N, Apte JS, Robinson AL, et al. 2018. Reduced ultrafine particle concentration in urban air: changes in nucleation and anthropogenic emissions. Environ Sci Technol 52(12):6798–6806, PMID: 29775285, https://doi.org/10.1021/acs.est.8b00910.

Samet JM, Dominici F, Curriero FC, Coursac I, Zeger SL. 2000. Fine particulate air pollution and mortality in 20 U.S. cities, 1987–1994. N Engl J Med 343(24):1742–1749, PMID: 11114312, https://doi.org/10.1056/NEJM200012143432401.

Saraswat A, Apte JS, Kandlikar M, Brauer M, Henderson SB, Marshall JD. 2013. Spatiotemporal land use regression models of fine, ultrafine, and black carbon particulate matter in New Delhi, India. Environ Sci Technol 47(22):12903–12911, PMID: 24087939, https://doi.org/10.1021/es401489h.

Seinfeld JH, Pandis SN. 2016. *Atmospheric Chemistry and Physics: From Air Pollution to Climate Change* Hoboken, NJ: John Wiley & Sons.

Shields LG, Suess DT, Prather KA. 2007. Determination of single particle mass spectral signatures from heavy-duty diesel vehicle emissions for $PM_{2.5}$ source apportionment. Atmos Environ 41(18):3841–3852, https://doi.org/10.1016/j.atmosenv.2007.01.025.

Sowlat MH, Hasheminassab S, Sioutas C. 2016. Source apportionment of ambient particle number concentrations in central Los Angeles using positive matrix factorization (PMF). Atmos Chem Phys 16(8):4849–4866, https://doi.org/10.5194/acp-16-4849-2016.

Squizzato S, Masiol M, Emami F, Chalupa DC, Utell MJ, Rich DQ, et al. 2019. Long-term changes of source apportioned particle number concentrations in a metropolitan area of the northeastern United States. Atmosphere (Basel) 10(1):27, https://doi.org/10.3390/atmos10010027.

Sullivan RC, Prather KA. 2005. Recent advances in our understanding of atmospheric chemistry and climate made possible by on-line aerosol analysis instrumentation. Anal Chem 77(12):3861–3886, PMID: 15952760, https://doi.org/10.1021/ac050716i.

Thurston GD, Burnett RT, Turner MC, Shi Y, Krewski D, Lall R, et al. 2016. Ischemic heart disease mortality and long-term exposure to source-related components of U.S. fine particle air pollution. Environ Health Perspect 124(6):785–794, PMID: 26629599, https://doi.org/10.1289/ehp.1509777.

Wilson MR, Lightbody JH, Donaldson K, Sales J, Stone V. 2002. Interactions between ultrafine particles and transition metals *in vivo* and *in vitro*. Toxicol Appl Pharmacol 184(3):172–179, PMID: 12460745, https://doi.org/10.1006/taap.2002.9501.

Wittig AE, Anderson N, Khlystov AY, Pandis SN, Davidson C, Robinson AL. 2004. Pittsburgh air quality study overview. Atmos Environ 38(20):3107–3125, https://doi.org/10.1016/j.atmosenv.2004.03.003.

Wittmaack K. 2007. In search of the most relevant parameter for quantifying lung inflammatory response to nanoparticle exposure: particle number, surface area, or what? Environ Health Perspect 115(2):187–194, PMID: 17384763, https://doi.org/10.1289/ehp.9254.

Ye Q, Gu P, Li HZ, Robinson ES, Lipsky EM, Kaltsonoudis C, et al. 2018. Spatial variability of sources and mixing state of atmospheric particles in a metropolitan area. Environ Sci Technol 52(12):6807–6815, PMID: 29775536, https://doi.org/10.1021/acs.est.8b01011.

Zelenyuk A, Imre D. 2005. Single particle laser ablation time-of-flight mass spectrometer: an introduction to SPLAT. Aerosol Sci Technol 39(6):554–568, https://doi.org/10.1080/027868291009242.

Zhang Q, Alfarra MR, Worsnop DR, Allan JD, Coe H, Canagaratna MR, et al. 2005. Deconvolution and quantification of hydrocarbon-like and oxygenated organic aerosols based on aerosol mass spectrometry. Environ Sci Technol 39(13):4938–4952, PMID: 16053095, https://doi.org/10.1021/es048568l.

Zhang Q, Jimenez JL, Canagaratna MR, Ulbrich IM, Ng NL, Worsnop DR, et al. 2011. Understanding atmospheric organic aerosols via factor analysis of aerosol mass spectrometry: a review. Anal Bioanal Chem 401(10):3045–3067, PMID: 21972005, https://doi.org/10.1007/s00216-011-5355-y.